

Subwavelength optical microscopy in the far field

Qingqing Sun,¹ M. Al-Amri,² Marlan O. Scully,^{1,3} and M. Suhail Zubairy¹

¹*Department of Physics and Institute of Quantum Studies, Texas A&M University, College Station, Texas 77843, USA*

²*The National Centre for Mathematics and Physics, KACST, P.O. Box 6086, Riyadh 11442, Saudi Arabia*

³*Princeton Institute for Materials Research, Princeton University, Princeton, New Jersey 08544-1009, USA*

(Received 28 November 2010; published 16 June 2011)

We present a procedure for subwavelength optical microscopy. The identical atoms are distributed on a plane and shined with a standing wave. We rotate the plane to different angles and record the resonant fluorescence spectra in the far field, from which we can obtain their distance and location information. This procedure also works for atomic separation above one wavelength and therefore provides a seamless microscopy.

DOI: [10.1103/PhysRevA.83.063818](https://doi.org/10.1103/PhysRevA.83.063818)

PACS number(s): 42.50.Ct, 42.30.-d

I. INTRODUCTION

High resolution optical microscopy is an important tool for many scientific fields. In the traditional far-field imaging, the light is collected through lens and diffraction limited by half of the optical wavelength [1]. One way to get around this obstacle is to use near-field scanning, where the evanescent wave is also collected to complete the information [2–4]. Nevertheless, people are still interested in far-field schemes with subwavelength resolution.

Many quantum optical methods have been proposed to go beyond the diffraction limit, including the two-photon imaging using entangled states for quantum lithography [5,6], photon correlations [7,8], two-photon fluorescence [9], and space-dependent dark states [10–14]. One method of particular interest is to use standing wave to drive an atom. Since the field intensity is space dependent, the location of the atom determines the drive field it feels, and consequently affects its dynamics. Therefore, the location information is encoded in many system observables [15–20]. If there are two identical atoms in the system, their separation can be extracted from the resonant fluorescence spectrum [21]. However, this scheme only works for two atoms in one dimension and within one wavelength.

In this paper, we extend the above scheme to a procedure of subwavelength optical microscopy. This procedure can (i) detect any number of atoms on a plane, (ii) provide both the locations and separation distances (the latter can be used to verify the locations), and (iii) work for both subwavelength and above wavelength ranges seamlessly, without the restriction from periodicity. In the next section, we describe our scheme and model in detail. In Sec. III, we discuss the analysis procedure to extract the information. Section IV is the summary.

II. SCHEME

The scheme we propose is shown in Fig. 1. The identical atoms are placed on a plane disk that can rotate around its center. We define a laboratory coordinate system (x, y, z) fixed in space, and a disk coordinate system (r', θ') fixed on the disk. The disk center is the origin for both coordinate systems. The disk rotation angle θ is the angle between the $\theta' = 0$ ray and the x axis. A resonant standing wave covers the whole disk with the Rabi frequency distribution $\Omega(x) = \Omega \sin(kx + \phi_0)$. The

collective fluorescence field is observed by a detector far away in the z direction. During the rotation, the disk coordinates (r'_i, θ'_i) of the i th atom do not change. However, the laboratory coordinate $x_i = r'_i \cos(\theta'_i - \theta)$ changes as a function of θ , and so do the local Rabi frequency $\Omega(x_i)$ and the spectrum. We record the spectrum for each angle. The result is a contour map that can uniquely determine the locations of the atoms. In this paper, we will numerically simulate these spectrum contours and then show the procedure to analyze them in different configurations.

For simplicity, we assume the transition dipole moments of all the atoms to be parallel and in the disk plane. The Hamiltonian of the system can be written as $H = H_0 + H_{dd} + H_L$. Here $H_0 = (\hbar\omega_0/2) \sum_{i=1}^N (S_i^+ S_i^- - S_i^- S_i^+)$ is the unperturbed Hamiltonian for the N atoms, with ω_0 being the level separation and S_i^+ (S_i^-) being the raising (lowering) operator for the i th atom. $H_L = (\hbar/2) \sum_{i=1}^N (\Omega_i S_i^+ e^{-i\omega_L t} + \text{H.c.})$ is the atom-field interaction part, where $\omega_L = \omega_0$ is the resonant field frequency. The dipole-dipole interaction $H_{dd} = \sum_{i \neq j} \hbar \Omega_{ij} (S_i^+ S_j^- + \text{H.c.})$, with the interaction strength given as

$$\Omega_{ij} = \frac{3}{2}\gamma \left\{ -\frac{\cos(kr_{ij})}{(kr_{ij})} + \frac{\sin(kr_{ij})}{(kr_{ij})^2} + \frac{\cos(kr_{ij})}{(kr_{ij})^3} \right\}, \quad (1)$$

where γ is the decay constant of the atoms and r_{ij} are the distance between atoms.

There are two types of decay terms in this system. Namely, the spontaneous emission rate for each atom $\gamma_{ii} = \gamma$ and the incoherent dipole-dipole couplings

$$\gamma_{ij} = \frac{3}{2}\gamma \left\{ \frac{\sin(kr_{ij})}{(kr_{ij})} + \frac{\cos(kr_{ij})}{(kr_{ij})^2} - \frac{\sin(kr_{ij})}{(kr_{ij})^3} \right\}. \quad (2)$$

With both the Hamiltonian and the decay terms at hand, we can write down the equation of motion for the density matrix ρ :

$$\dot{\rho} = -\frac{i}{\hbar}(H, \rho) - \sum_{i,j=1}^N \gamma_{ij} [(S_i^+, S_j^- \rho) - (S_j^-, \rho S_i^+)]. \quad (3)$$

The solution allows us to find the single-time correlation functions. Then, from quantum regression theorem, we derive

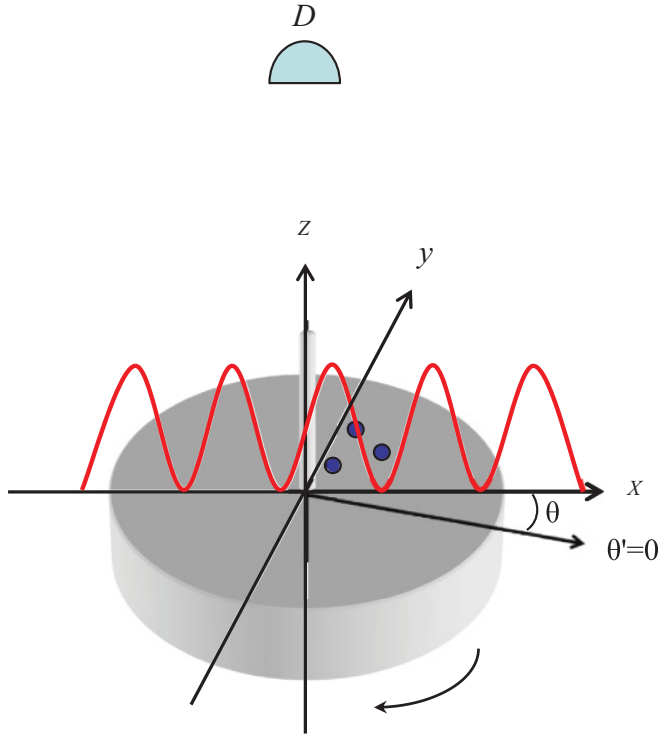


FIG. 1. (Color online) Microscopy scheme. The atoms are on the disk submerged in the standing wave. The analysis of the collective fluorescence spectra at different rotation angles reveals the atomic locations, even if they are within subwavelength distance.

the two-time correlation functions, which finally lead to the resonance fluorescence spectrum,

$$S(\omega) = \text{Re} \int_0^\infty d\tau e^{i(\omega - \omega_L)\tau} \sum_{i,j=1}^N \langle S_i^+(0) S_j^-(\tau) \rangle e^{ik\hat{R}\cdot r_{ij}}, \quad (4)$$

where the observation direction \hat{R} is along the z axis.

III. RESULTS AND DISCUSSIONS

The dipole-dipole interaction depends on the distance between two atoms. It is very sensitive when the atoms are close to each other. So we categorize the configurations based on the ranges of the distances. As the simplest multiatom cases, we discuss the various configurations for two or three atoms.

A. All atoms far separated

For an atom far away from all the others, its dipole-dipole interaction with the other atoms is negligible. So its dynamics is the same as a single, independent atom. It is well known that for a two-level atom interacting with a single mode field, the resonant fluorescence spectrum has a central peak at zero detuning, as well as two sideband peaks at $\pm|\Omega(x)|$. The sideband detuning gives us the local Rabi frequency, from which we can retrieve x [21]. However, for a standing wave, within one wavelength there are four x coordinates that have the same $|\Omega(x)|$. The duplicity is even worse due to the wave periodicity. Another issue of the single spectrum method is it does not provide any information about the y coordinate.

In our proposed method, we can uniquely determine the disk coordinates (r'_i, θ'_i) of the i th atom. As the disk rotates, the sideband peak at $|\Omega \sin[kr'_i \cos(\theta'_i - \theta) + \phi_0]|$ moves continuously and forms a curve as a function of θ . This curve is unique for each location (r', θ') as far as the predetermined phase $\phi_0 \neq 0$. Otherwise, the curve would be the same for

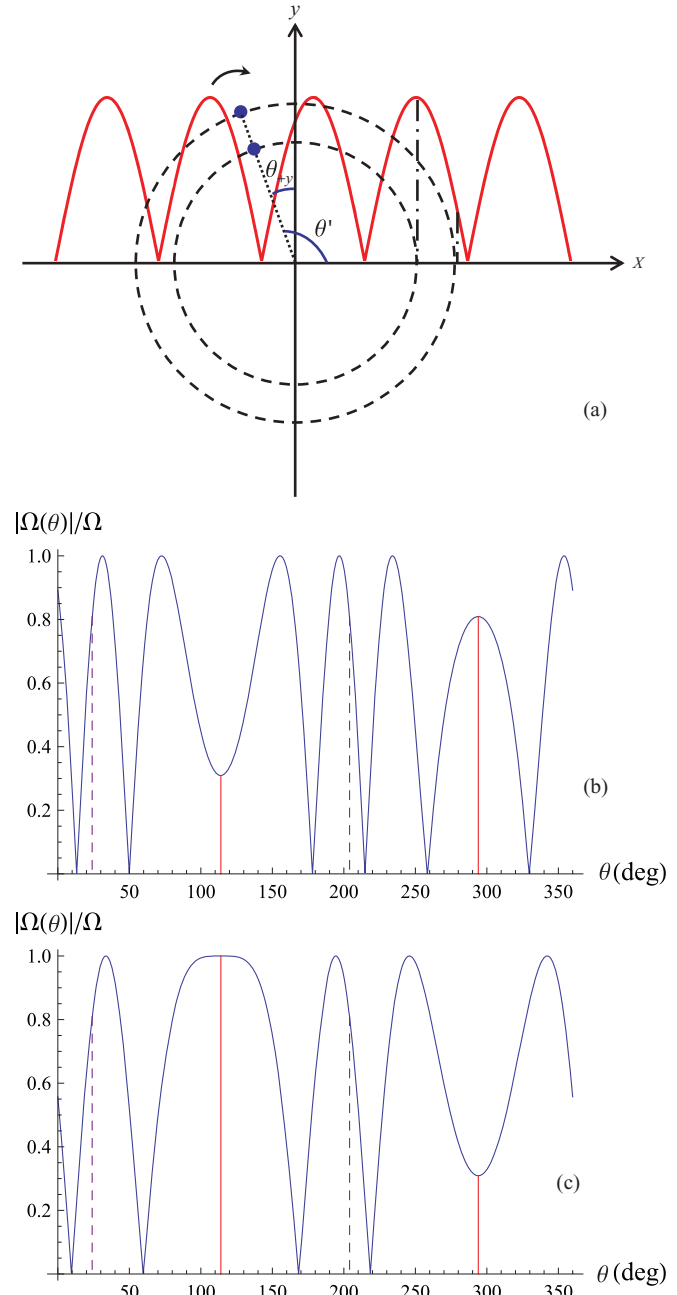


FIG. 2. (Color online) (a) Atoms rotate with the disk. (b) The typical sideband peak curve, drawn from the outer atom. Red lines correspond to the angles where the atom crosses the x axis and purple dashed lines correspond to the angles where the atom crosses the y axis. (c) The sideband peak curve when one of the local extreme is Ω , drawn from the inner atom. We can still find the extreme angles from the other local extreme.

atoms at (r', θ') and $(r', \theta' + \pi)$. We can further assume $0 < \phi_0 < \pi/2$ without loss of generality.

To analyze this sideband peak curve, we need to understand its typical features first. As shown in Fig. 2, the atom crosses the x axis twice during one circle of disk rotation. At these two angles, x_i approaches the extreme values $\pm r'_i$ and then goes back. So $|\Omega(x_i)|$ reaches a local minimum or maximum, usually neither 0 nor Ω . These two extreme angles are separated by π . Similarly, the atom crosses the y axis twice at angles $\pi/2$ from the extreme angles. When the atom crosses the $+y$ axis, we should see the rising trend of $|\Omega(\theta)|$ due to $0 < \phi_0 < \pi/2$.

The analysis procedure goes as follows: on the sideband peak curve, we mark the two extreme angles and then mark the two angles $\pi/2$ from them as the vertical angles. The vertical angle with a rising trend θ_{+y} is where the atom crosses the $+y$ axis. The atom crosses the $+x$ axis at $\theta_{+y} + \pi/2$, which is equal to its disk coordinate θ'_i . When the atom rotates from $+y$ axis to $+x$ axis, its laboratory coordinate x_i increases from 0 to r'_i , during which the sideband detuning encounters Ω and 0 alternatively until it reaches the local extreme. If there are p number of Ω s and p number of 0s, we can find $kr'_i = p\pi + \arcsin[|\Omega(\theta_{+y} + \pi/2)|/\Omega] - \phi_0$. If the number of 0s is instead $p - 1$, then $kr'_i = p\pi - \arcsin[|\Omega(\theta_{+y} + \pi/2)|/\Omega] - \phi_0$.

We simulate the spectrum contour of two atoms far separated from each other, as shown in Fig. 3. In this contour, each vertical line corresponds to the positive half spectrum at a certain rotation angle. The spectrum intensity is indicated by the color. The peak curves agree with the local Rabi frequency curves (on top) experienced by the atoms quite well, which verifies the dominance of the Rabi frequency and the

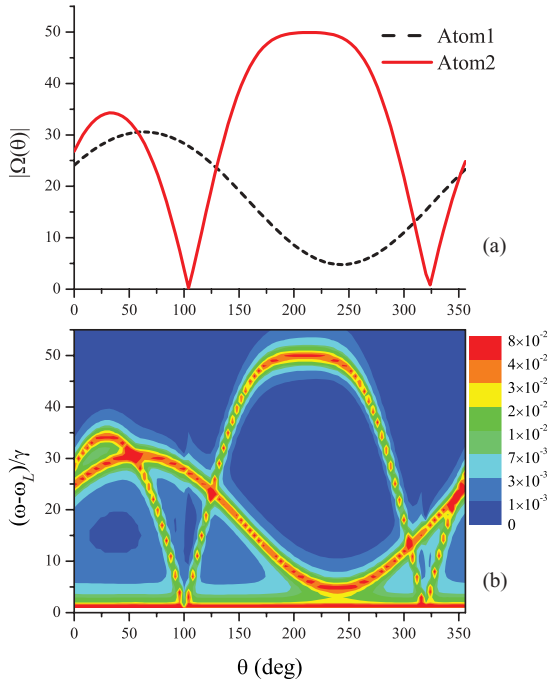


FIG. 3. (Color online) Two atoms far from each other. $\phi_0 = 0.06 \times 2\pi$, $x'_1 = 0.02\lambda$, $y'_1 = 0.04\lambda$, $x'_2 = -0.15\lambda$, $y'_2 = -0.1\lambda$, and $\Omega = 50\gamma$. (a) The local Rabi frequency curves for the atoms. (b) The spectrum contour.

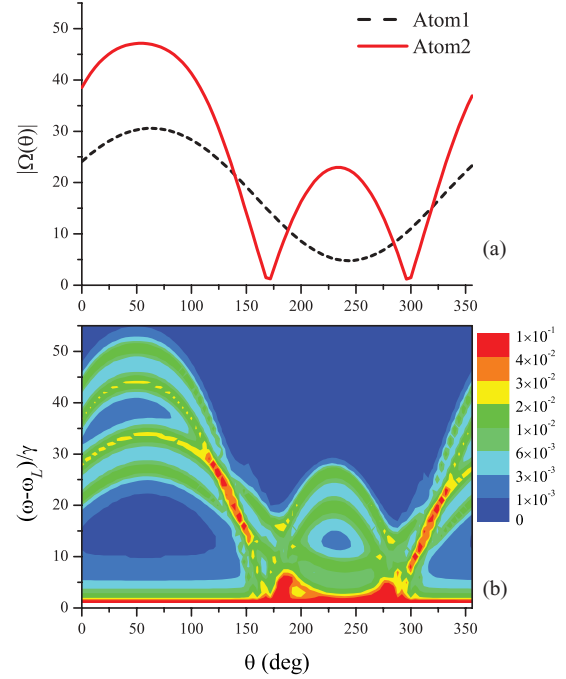


FIG. 4. (Color online) Two atoms in the medium range. $\phi_0 = 0.06 \times 2\pi$, $x'_1 = 0.02\lambda$, $y'_1 = 0.04\lambda$, $x'_2 = 0.08\lambda$, $y'_2 = 0.11\lambda$, and $\Omega = 50\gamma$. (a) The local Rabi frequency curves for the atoms. (b) The spectrum contour.

independence of these atoms. From the above procedure, we can easily find the coordinates used for simulation.

B. Two atoms in medium range

The next situation we consider is when two atoms are within the medium range (0.08λ to 0.03λ). The simulated contour map is shown in Fig. 4. The dipole-dipole interaction is larger than the decay and becomes noticeable. It splits each sideband peak into a pair of peaks so there are two pairs of curves. These pairs have the same internal split $2\Omega_{12}$ at most angles (when $\Omega_1, \Omega_2 \gg \gamma$), and each pair joins together near zero Rabi frequency because there the dipole-dipole interaction is dominant and no longer splits the curve. The average of each pair matches a local Rabi frequency curve. So we can find the location of these atoms by taking the average of a pair and analyzing it just like an independent atom.

C. Two atoms close

When two atoms are close to each other, they have a strong dipole-dipole interaction with the strength Ω_{12} much greater than decay. If the strength is also much larger than the Rabi frequency, then it becomes dominant. In that case, the spectrum has a sideband peak located at Ω_{12} , which only depends on the distance between the atoms and does not change when we rotate the disk, as we can see from Fig. 5. When we increase the Rabi frequency, that dipole-dipole peak starts to split.

The constant sideband detuning does not provide information about the local Rabi frequency. Nevertheless, we can find this information from the peak height, which depends on the population of the excited level. In a strong drive field, half of the population is excited and the peak height is independent

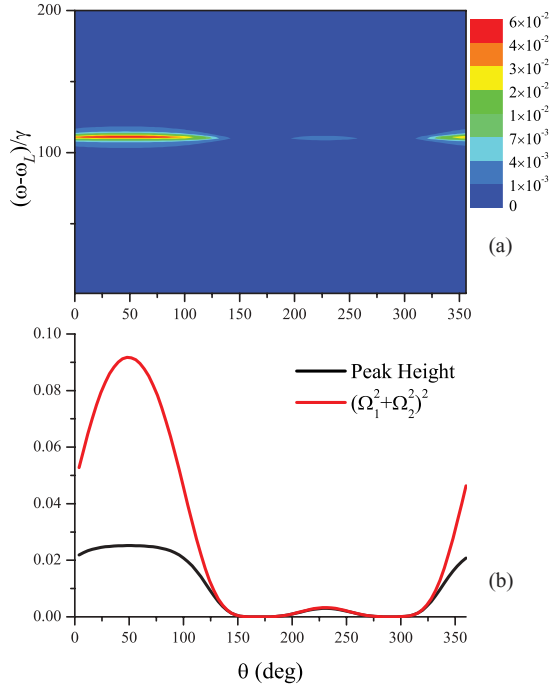


FIG. 5. (Color online) Two atoms close together. $\phi_0 = 0.06 \times 2\pi$, $x'_1 = 0.08\lambda$, $y'_1 = 0.08\lambda$, $x'_2 = 0.08\lambda$, $y'_2 = 0.11\lambda$, and $\Omega = 20\gamma$. (a) The spectrum contour. (b) The peak height curve is proportional to $(\Omega_1^2 + \Omega_2^2)^2$ for weak intensity.

of the local Rabi frequency. However, in a weak drive field, the excited population is linear to $\Omega_1^2 + \Omega_2^2$. Therefore, the peak height is proportional to $(\Omega_1^2 + \Omega_2^2)^2$, as shown in Fig. 5. Since we already know the separation between the atom pair, we can perform a data fitting with three unknown variables: two coordinates of the first atom and its angle with the second atom.

D. Three atoms close

When all three atoms are close to each other, there are three dipole-dipole interactions. Their interplay determines the peak curves. So the location of any peak curve no longer reveals the distance between two atoms. However, we can still treat this problem with contour analysis.

The typical feature of the contour is that there are three lowest groups of peak curves and the others are their combinations, as shown in Fig. 6. The peak locations are the eigenvalues of the Hamiltonian. When all local Rabi frequencies are zero, there are three nonzero eigenvalues $2p \cos \beta$, $2p \cos(\beta + 2\pi/3)$, and $2p \cos(\beta + 4\pi/3)$, where $p = \sqrt{(\Omega_1^2 + \Omega_2^2 + \Omega_3^2)/3}$. So when

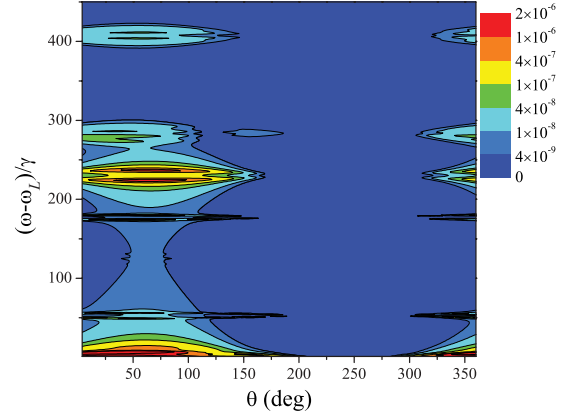


FIG. 6. (Color online) Spectrum contour for three close atoms. The lowest three peak curves provide the dipole-dipole information. The other curves are just their combinations.

the atoms are at the minimum of the standing wave, the peak locations give us the information about p .

When the atoms are at the maximum of the standing wave, the Rabi frequencies split the eigenvalues and the peaks. We choose the peak Rabi frequency to be large enough for splitting, but much smaller than dipole-dipole interactions so it is just a perturbation, say $\Omega = 10\gamma$. The splittings plus the known p allow us to perform data fitting to get Ω_{ij} . If the peak locations can be measured within the accuracy of 0.1γ , the fitting error is within a few γ . Then we can find r_{ij} from Ω_{ij} . With all the r_{ij} , we obtain the configuration of the three atoms. The only unknown parameters are the location of the first atom and the orientation of the whole configuration relative to that atom, which in principle can be determined from another data fitting. A similar method can be applied to N close atoms.

IV. SUMMARY

We propose a general procedure of subwavelength optical microscopy using resonant fluorescence spectrum. This method can uniquely determine the locations of many atoms on a two-dimensional plane, and is not limited to one wavelength. We analyze various configurations for two or three atoms and these procedures can be generalized to cases with more atoms.

ACKNOWLEDGMENTS

This work is supported by a grant from the King Abdul Aziz City for Science and Technology (KACST) and the Qatar National Research Fund (QNRF) under a NPRP grant.

- [1] Lord Rayleigh, *Philos. Mag.* **8**, 261 (1879).
 [2] A. Lewis, M. Isaacson, A. Harootuniana, and A. Muraya, *Ultramicroscopy* **13**, 227 (1984).
 [3] E. Betzig, *Opt. Lett.* **20**, 237 (1995).
 [4] C. Hettich, C. Schmitt, J. Zitzmann, S. Kühn, I. Gerhardt, and V. Sandoghdar, *Science* **298**, 385 (2002).

- [5] A. N. Boto, P. Kok, D. S. Abrams, S. L. Braunstein, C. P. Williams, and J. P. Dowling, *Phys. Rev. Lett.* **85**, 2733 (2000).
 [6] M. D'Angelo, M. V. Chekhova, and Y. Shih, *Phys. Rev. Lett.* **87**, 013602 (2001).
 [7] M. O. Scully and C. H. Raymond Ooi, *J. Opt. B: Quantum Semiclass. Opt.* **6**, S816 (2004).

- [8] A. Muthukrishnan, M. O. Scully, and M. S. Zubairy, *J. Opt. B: Quantum Semiclass. Opt.* **6**, S575 (2004).
- [9] W. Denk, J. H. Strickler, and W. W. Webb, *Science* **248**, 73 (1990).
- [10] S. Bretschneider, C. Eggeling, and S. W. Hell, *Phys. Rev. Lett.* **98**, 218103 (2007).
- [11] D. D. Yavuz and N. A. Proite, *Phys. Rev. A* **76**, 041802(R) (2007).
- [12] A. V. Gorshkov, L. Jiang, M. Greiner, P. Zoller, and M. D. Lukin, *Phys. Rev. Lett.* **100**, 093005 (2008).
- [13] M. Kiffner, J. Evers, and M. S. Zubairy, *Phys. Rev. Lett.* **100**, 073602 (2008).
- [14] H. Li, V. A. Sautenkov, M. M. Kash, A. V. Sokolov, G. R. Welch, Y. V. Rostovtsev, M. S. Zubairy, and M. O. Scully, *Phys. Rev. A* **78**, 013803 (2008).
- [15] P. Storey, M. Collett, and D. F. Walls, *Phys. Rev. Lett.* **68**, 472 (1992).
- [16] S. Kunze, K. Dieckmann, and G. Rempe, *Phys. Rev. Lett.* **78**, 2038 (1997).
- [17] F. Le Kien, G. Rempe, W. P. Schleich, and M. S. Zubairy, *Phys. Rev. A* **56**, 2972 (1997).
- [18] A. M. Herkommer, W. P. Schleich, and M. S. Zubairy, *J. Mod. Opt.* **44**, 2507 (1997).
- [19] H. Nha, J.-H. Lee, J.-S. Chang, and K. An, *Phys. Rev. A* **65**, 033827 (2002).
- [20] S. Qamar, S.-Y. Zhu, and M. S. Zubairy, *Phys. Rev. A* **61**, 063806 (2000).
- [21] J.-T. Chang, J. Evers, and M. S. Zubairy, *Phys. Rev. A* **74**, 043820 (2006).